Engineering Notes

ENGINEERING NOTES are short manuscripts describing new developments or important results of a preliminary nature. These Notes cannot exceed 6 manuscript pages and 3 figures; a page of text may be substituted for a figure and vice versa. After informal review by the editors, they may be published within a few months of the date of receipt. Style requirements are the same as for regular contributions (see inside back cover).

Modularized Ion Thruster Development for Auxiliary Propulsion

J. Hyman Jr.* and C. R. Dulgeroff†
Hughes Research Laboratories, Malibu, Calif.

Introduction

A FAMILY of modularized mercury ion thrusters has been developed[1] which extends the operational capability of a 1-mlb engineering model thruster[2] (EMT) by employing interchangable discharge chamber modules (DCM's) that have been optimized for efficient operation at nominal thrust levels of 0.5, 1, and 2 mlb. Preliminary data have also been obtained for operation at the 4-mlb thrust level. Only the discharge chamber and beam-extraction system have been modified under this development. As shown in Fig. 1, all of the critical subassemblies of the module support system (MSS) are identical with those in the highly developed 1-mlb EMT; these include the cathode-isolator-vaporizer (CIV), neutralizer-isolator-vaporizer (NIV), gimbal mounting structure, and the aperture pattern of the beam-extraction system.

Operation at the 0.5-mlb thrust level provides an attractive alternative to 1-mlb operation for low-impulse propulsion applications where the peak power level is limited. Operation at the higher thrust levels has been motivated by the recent advent of an efficient lightweight nickel-hydrogen (Ni-H) battery, which has been proposed as a power source for satellite control thrusters.[3] The Ni-H/ion-propulsion combination permits operation at higher power and thrust levels without requiring unacceptable peak-power loading of the solar-panel power source. Operation at increased thrust levels reduces the necessary beam-on time below the maximum value of 20,000 required for a 7-yr mission. This reduction is expected to have a positive impact on the acceptance of electric propulsion systems by potential users who now express concern over present thruster lifetime requirements.[4]

System Description

In the modularized ion thruster development, efficient thruster performance has been demonstrated over a range of thrust levels. This goal has been accomplished using CIV and NIV subassemblies identical to those employed in the 1-mlb EMT design configuration.[2] No essential change has been required in the overall structural configuration for operation at any of four thrust levels. (0.5, 1.0, 2, or 4 mlb), except that a larger-size ground-screen enclosure is employed to accomodate the larger size of the DCM's used for operation at thrust levels $T=2$mlb and $T=4$ mlb; the gimbal adapter and other support members are only slightly affected by this difference. To complete the system assembly, a particular DCM module of the chosen thrust level is attached to the MSS by bolting the DCM endplate flange to the four DCM support insulators and mating the endplate with CIV subassembly.

Critical dimensions for the three new DCM designs are shown in Table 1; dimensions of the 1-mlb EMT are also

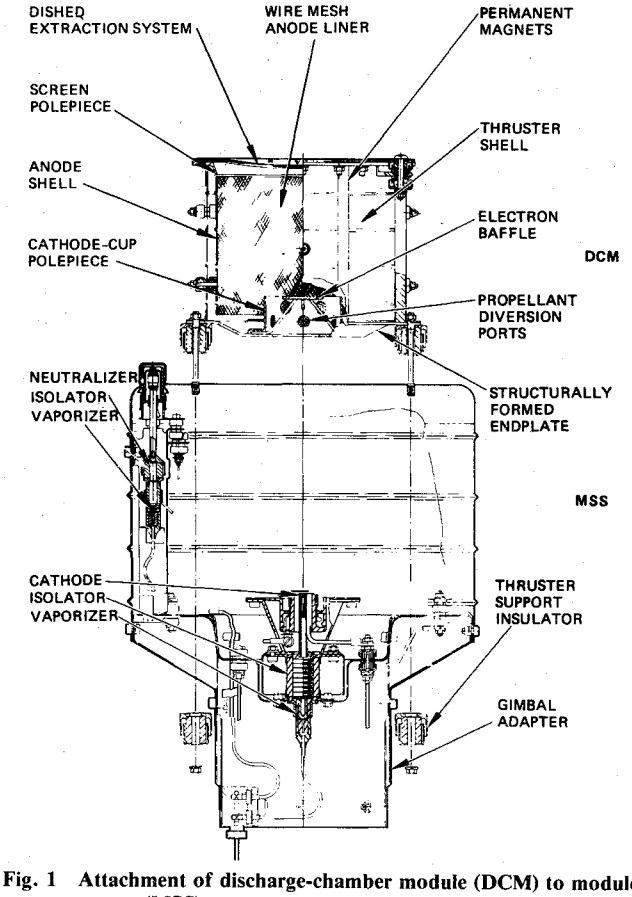

Fig. 1 Attachment of discharge-chamber module (DCM) to module support system (MSS).

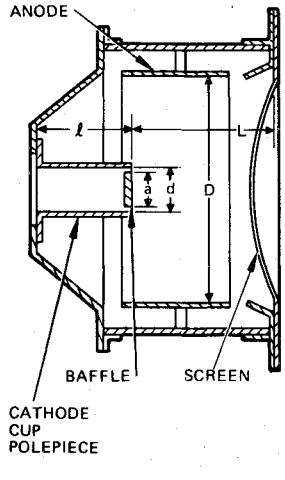

Fig. 2 Cross-sectional sketch of DCM geometry showing terms used in Table 1.

Presented as Paper 76-1049 at the AIAA International Electric Propulsion Conference, Key Biscayne, Fla., Nov. 14-17, 1976; submitted Jan. 4, 1977; revision received Oct. 6, 1977.

Index category; Electric and Advanced Space Propulsion.

*Head, Plasma Research Section, Ion Physics Department. Associate Fellow AIAA.

†Senior Staff Physicist, Ion Physics Department.

Table 1 DCM critical dimensions

	0.5 mlb thrust level	1 mlb thrust level	2 mlb thrust level	4 mlb thrust level
Thruster body assembly				
Effective discharge chamber length (L), mm	67	67	113	117
Diameter of anode (D), mm	86	86	144	144
Length of cathode-cup-polepiece (l), mm	17	17	21	21
Inside diameter of cathode-cup polepiece (d), mm	38	38	43	43
Transparancy of cathode-cup enclosure surface, %	0	8	24.8	24.8
Baffle diameter (a), mm	18	21	26	29
Number of magnets (0.485 cm diameter)	8	8	16	16
Mass of DCM plus MSS, kg	1.838	2	3.338	[a]
Beam extraction system				
Electrode-dish radius of curvature, mm	300	300	450	450
Accel aperture diameter, mm	0.7	1.1	1.0	1.0

[a] Optimization not complete.

included for reference purposes. The nomenclature used in Table 1 is defined by the cross-sectional sketch of the DCM geometry shown in Fig. 2. For the 2- and 4-mlb thrust levels, the cathode-cup enclosure has been penetrated to provide propellant-diversion ports which lower the neutral-particle density in the vicinity of the main cathode, so as to adjust discharge-chamber impedance to the desired value.[5] The portholes are covered by a 49%-transparent tantalum-wire mesh (0.008-cm wire diameter) which is brazed to the inside of the cathode cup; this mesh interrupts the continuity of plasma flow and restricts the transmission of electron current to the region of an annular gap between the electron baffle and the lip of the cathode-cup polepiece. In the preliminary test at 4-mlb thrust level, an additional 30% of the propellant was diverted through the endplate of the discharge chamber. The individual beam-extraction systems which were used for optimization of the three separate DCM's had many common dimensions, i.e., center-to-center aperature spacing = 2.2mm, screen aperature diameter = 1.9mm, interelectrode spacing = 0.8 mm, accel thickness = 0.4mm, and screen thickness = 0.3mm. Although the spacings and apertures were the same for the 1-mlb EMT as for the DCM's, the 1-mlb EMT accel and screen electrodes were 0.1mm thicker.

In preparation for optimization tests, the aperatures of the accel electrodes were chemically machined by a photo-etch process to a size close to that of the final chosen dimension. In the final configuration of the 0.5 and 2-mlb DCM's however, the beam-extraction systems for the individual DCM's were custom-fitted by ion-machining of the accel aperatures.[6] A significant improvement in discharge-chamber utilization (over the values obtained in the optimization tests) was obtained with the somewhat smaller ion-machined apertures.

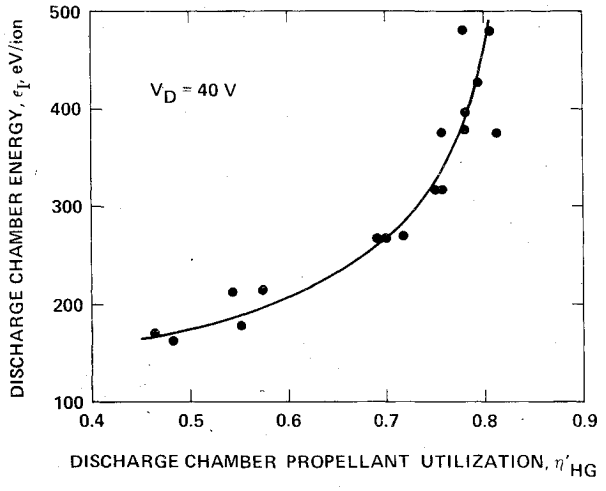

Fig. 3 Discharge specific energy ϵ_I as a function of discharge chamber propellant utilization η'_{Hg} for 0.5-mlb optimized DCM.

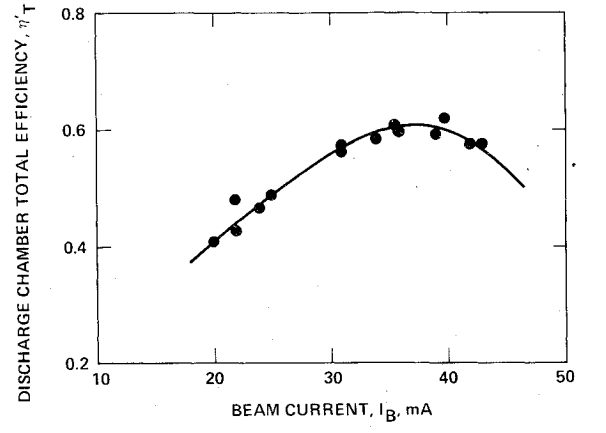

Fig. 4 Discharge-chamber total efficiency η'_T as a function of beam current I_B for 0.5-mlb optimized DCM.

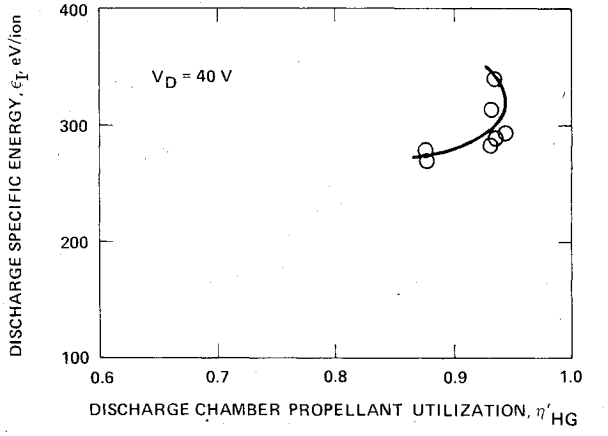

Fig. 5 Discharge specific energy ϵ_I as a function of discharge-chamber propellant utilization η'_{Hg} for 2-mlb optimized DCM.

Table 2 DCM performance

	0.5 mlb[a]	1.0 mlb[a]	2.0 mlb[a]	4.0 mlb 03b (preliminary)
Thrust, mlb	0.58	1.10	2.23	5.1
Specific impulse, s	2676	2801	2980	3729
Total input power, W	70.8	125	234.9	587.9
Total efficiency, %	48.0	55.3	65.5	70.2
Power efficiency, %	61.2	69.0	73.6	73.0
Total utilization, %	78.5	80.2	89.1	96.2
Discharge utilization, %	90.4	85.8	93.3	98.1
Total neutral flow, mA	45.3	85.3	154.6	297.4
Power/thrust, W/mlb	124.2	112.6	105.3	116
eV/ion including keeper, V	226	335	267	421
Beam current (I_B), mA	36	72	144	286
Anode-to-neutralizer tip potential (V_B), V	1215	1205	1220	1500
Neutralizer coupling potential (V_N), V	−12	−7.8	−20	−20[c]
Output beam power, W	43.3	86.2	172.8	429
Accelerator voltage (V_A), V	−100	−300	−100	−280
Accelerator drain current (I_A), mA	0.4	0.24	1.5	2
Accelerator drain power, W	0.04	0.01	0.02	0.06
Discharge voltage (V_D), V	40	40	40	40
Discharge current (I_D), A	0.160	0.565	0.880	2.95
Discharge power, W	6.4	22.6	35.2	118
Discharge:				
Keeper voltage (V_{DK}), V	10.5	5.1	9.1	8.0
Keeper current (I_{DK}), A	0.150	0.1	0.35	0.30
Keeper power, W	1.6	0.5	3.19	2.4
Heater voltage (V_{DH}), V	0	0	0	0
Heater current (I_{DH}), A	0	0	0	0
Heater power, W	0	0	0	0
Vaporizer voltage (V_{DV}), V	4.8	4.55	4.8	3.9
Vaporizer current (I_{DV}), A	1.85	1.58	1.9	1.9
Vaporizer power, W	8.9	7.2	9.12	7.4
Flow rate (I_{DHg})	39.3	79.7	149.6	291.4
Neutralizer:				
Keeper voltage (V_{NK}), V	21	13.2	13	20[c]
Keeper current (I_{NK}), A	0.350	0.5	0.620	1.0[c]
Keeper power, W	7.4	6.6	8.06	20[c]
Heater voltage (V_{NH}), V	0	0	0	0
Heater current (I_{NH}), A	0	0	0	0
Heater power, W	0	0	0	0
Vaporizer voltage (V_{NV}), V	2.6	1.8	2.1	3.6[c]
Vaporizer current (I_{NV}), A	0.9	0.5	0.8	0.5[c]
Vaporizer power, W	2.3	0.9	1.68	1.8[c]
Flow rate (I_{NHg})	6	5.6	5	6[c]
Neutralizer coupling power, W	0.4	0.6	2.88	5.7[c]

[a] Accounting for neutralizer floating potential V and effects due to beam divergence and the presence of doubly charged ions.

[b] Accounting for neutralizer floating potential V, but neglecting effects due to beam divergence and the presence of doubly charged ions.

[c] Instrumentation did not permit measurement of coupling values. Best estimates were made for neutralizer operation.

DCM Optimization Techniques

At present only the 0.5- and 2-mlb DCM's have been fully optimized; optimization of the 4-mlb DCM is only preliminary. Optimitation techniques and procedures described in the following discussion therefore, pertain specifically to operation of the 0.5 and 2-mlb DCM's

During the optimization phase, each thruster was equipped with a remotely movable cathode, variable electromagnets, and a conventional beam-extraction system. During the final stages of optimization, fixed permanent magnets and a fixed cathode were intalled. Two anode diameters were evaluated for each DCM. With each anode diameter, the DCM was optimized with respect to variations in effective discharge-chamber length, cathode-cup-polepiece length, cathode-cup-polepiece open-wall area, baffle diameter, axial cathode position, and magnetic field.

Throughout the optimization testing, the most desirable operating point was determined on the basis of the best operating stability, lowest discharge energy per beam-ion ϵ_I, and highest discharge-chamber propellant utilization η'_{Hg}, as a function of cathode position, electromagnet current, and main-keeper current. The primary figure of merit chosen for selection of a better configuration was the discharge-chamber efficiency η'_T, which is defined as the product of the discharge-chamber electrical efficiency η'_E and the discharge-chamber propellant utilization efficiency η'_{Hg}. These definitions exclude from consideration the fixed heater and neutralizer losses, since these parameters were not being optimized as part of this development. The relative propellant-utilization efficiency of alternative operating points was evaluated initially on the basis of the discharge-vaporizer temperature. Best point data determined from vaporizer temperature were subsequently

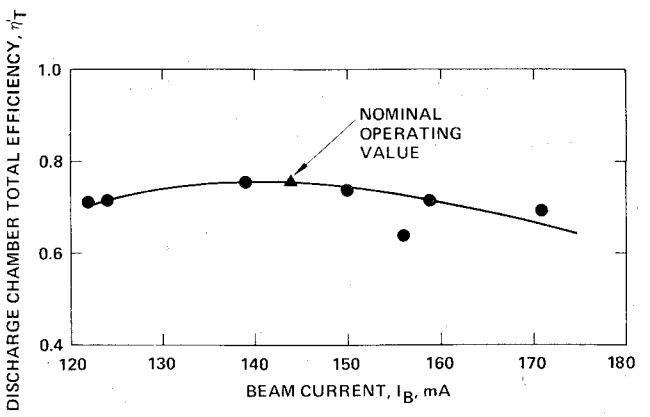

Fig. 6 Discharge-chamber total efficiency η_T' as a function of beam current I_B for 2-mlb optimized DCM.

confirmed by obtaining a mercury flowrate measurement from volumetric displacement of a liquid column over a 1-h period. Discharge-chamber performance for a given configuration was characterized for operation over the range in discharge voltage $37V \leq V_D \leq 40V$ and over a range of discharge current values (determined by discharge stability) with $V_D = 40V$.

The basic geometry of the 2-mlb DCM has also been tentatively chosen for operation at the thrust level $T = 4$ mlb with performance modifications resulting mainly from a change in the method of delivery of mercury vapor to the discharge chamber. In the present 4-mlb DCM configuration, approximately 30% of the mercury-vapor flow is transmitted through a diffuser plate located between the end of the discharge chamber and the base of the cathode-cup polepiece. Thus far, no optimization of discharge-chamber size or magnetic field shape or intensity has been attempted and only preliminary optimization has been attempted with regard to cathode position or in selection of electron baffle size and diffuser plate design.

DCM Performance

The results of the 0.5-mlb DCM optimization tests are shown in Figs. 3 and 4. In Fig. 3, the discharge specific energy ϵ_I is plotted as a function of discharge-chamber propellant utilization efficiency η_{Hg}'. The utilization efficiency reaches a maximum value of $\eta_{Hg}' \approx 80\%$. In Fig. 4, the discharge-chamber total efficiency η_T' is shown as a function of a beam current I_B; discharge-chamber total efficiency reaches a maximum value for beam currents in the range $35\,mA \leq I_B \leq 40mA$.

The results of the 2-mlb DCM optimization tests are shown in Figs. 5 and 6. Figure 5 shows that discharge-chamber propellant utilization reaches a maximum of 93%; Figure 6 shows that total discharge-chamber efficiency η_T' varies only slightly over the range of beam-current values recorded.

Table 2 summarizes performance of the three DCM's in their final configurations with ion-machined accel apertures, Performance of the l-mlb EMT with chemically machined accel electrode is also included for reference. For the 0.5-mlb DCM with the ion-machined apertures, discharge-chamber propellant utilization is significantly higher than the values obtained with photo-etched apertures shown in Fig. 3. This difference is not as pronounced for the 2-mlb DCM, however, since the aperture diameters of the 2-mlb DCM ion-machined optics were nearly identical to the 2-mlb DCM photo-etched apertures.

Conclusions

An efficient method has been developed for scaling the thrust level of an ion thruster by use of separate discharge-chamber modules while retaining all critical subassemblies of the basic system design.[1] This scaling has been demonstrated in the range of thrust levels from 0.5-4.0 mlb.

Acknowledgment

This work was supported in part by the NASA Lewis Research Center under NASA Contract NAS 3-19691. Technical development was carried out at Hughes Research Laboratories in cooperation with the Small Thruster Section of the Electric Propulsion Branch of NASA Lewis Research Center.

References

[1] Hyman, J. Jr. and Dulgeroff, C. R., "Modularized Ion Thruster," Hughes Research Labs., Malibu, Calif., Final Rept. on NASA Contract NAS 3-19691 NASA CR134667, 1976.

[2] Herron, B. G., Hyman, J. Jr., and Hopper, D. J., "8-cm Engineering Model Thruster Development," AIAA Paper 76-1058, AIAA 12th Electric Propulsion Conference, Key Biscayne, Fla., Nov. 1976.

[3] Free, B. A., "Electric Propulsion Technology Status and Development Plans: Commercial Satellite Programs," AIAA Paper 73-1145, AIAA 10th Electric Propulsion Conference, Lake Tahoe, Nev., Oct.-Nov. 1973.

[4] Mitchell, D. H. and Huberman, M. N., "Ion Propulsion for North-South Stationkeeping of Communication Satellites," AIAA Paper 76-290, AIAA/CASI 6th Coomunications Satellite Systems Conference, Montreal, Can., April 1976.

[5] Hyman, J. Jr. and Poeschel, R. L., "Satellite Control Mercury Ion Thruster," AIAA Paper 73-1132, AIAA 10th Electric Propulsion Conference, Lake Tahoe, Nev., Oct-Nov. 1973.

[6] Hudson, W. R., "Auxiliary Propulsion Thruster Performance with Ion-Machined Accelerator Grids," AIAA Paper 75-425, AIAA 11th Electric Propulsion Conference, New Orleans, La. March 1975.

Approximate Velocity of Bodies Powered by Cold-Gas Thrusters with Small Propellant Mass

M. D. Bennett*
Sandia Laboratories, Albuquerque, N. Mex.

Nomenclature

b	= mass-fraction parameter $= \lambda/(1-\lambda)$
c_i	= initial speed of sound in propellant gas, m/s
I_s	= thruster specific impulse, m/s
k	= specific-heats parameter $= 2/(\gamma-1)$
m_f	= vehicle final mass, kg
m_i	= vehicle initial mass, including propellant gas, kg
R	= gas constant, J/kg − K
T_i	= gas initial temperature, K
v_{max}	= vehicle terminal velocity, m/s
γ	= ratio of specific heats of ideal gas
ζ	= specific-heats factor $= (\gamma+1)/(\gamma-1)$
θ	= specific-heats term $= [2/(\gamma+1)][2/(\gamma-1)]^{1/2}$
λ	= vehicle mass fraction $= m_f/m_i$

Introduction

SEVERAL previous investigations of the translational motion of a missile discharging an inert propulsive gas from a thermally insulated tank involved an integral equation

Received Jan. 19, 1978.

Index categories: Missile Systems; Fuels and Propellants, Properties of.

*Member of Technical Staff, Aerodynamics Department. Associate Fellow AIAA.